

Cow Urine Mediated Synthesis of CeO₂ Nanoparticles for Display and Latent Fingerprints Application

H. J. Amith Yadav ^{1,*} , B. Eraiah ², M. N. Kalasad ¹, Vijay Kumar R ¹, Madhura S ¹, Nisha S ¹, Srinidhi K.S. ¹

¹ Department of Studies in Physics, Davangere University, Davangere 577007, India

² Department of Physics, Bangalore University, Bangalore 560056, India

* Correspondence: amithyadavhj@gmail.com(H.J.A.Y.);

Scopus Author ID 57021721300

Received: 12.06.2023; Accepted: 7.01.2024; Published: 28.08.2024

Abstract: The CeO₂ nanoparticles were synthesized using a combustion method using cow urine as fuel. The structural and morphological properties of CeO₂ nanoparticles were characterized by Powder X-ray diffraction (PXRD), Diffuse reflectance spectroscopy(DRS), Photoluminescence (PL), and TEM. PXRD results confirm the formation of the cubic phase. The energy band gap determined by Kubelka-Munk was found to be 3.1eV. The Commission Internationale de l'Eclairage (CIE) coordinates were located in the blue region. The synthesized CeO₂ nanoparticles can be used to develop latent fingerprints.

Keywords: cerium oxide; cow urine; combustion synthesis; display application.

© 2024 by the authors. This article is an open-access article distributed under the terms and conditions of the Creative Commons Attribution (CC BY) license (<https://creativecommons.org/licenses/by/4.0/>).

1. Introduction

In recent years, much research has been done on Nanomaterials [1]. Nanomaterials have unit sizes between 1 and 100nm. Due to their high surface-to-volume ratio, the nanoparticles have a variety of physical and chemical properties [2]. In the last few decades, nanotechnology applications have made advancements in fuel cells[3], vaccines, polishing agents, batteries[4], construction materials[5], displays, and forensic applications.

Due to their superior applications—energy harvesting, long life, and eco-friendliness—wLEDs (white light-emitting diodes) are replacing modern bright and luminous lamps. At the moment, the development of luminescent resources has attracted physics scientists. Inorganic compounds, especially, have been generally used in a variety of applications; for instance, field discharge shows radiation dosimetry, cathode beam tubes (CRTs), and light-emitting diodes (LEDs). Amid these, the wLEDs have been drawn in additional in the new times attributable to their energy saving, less harmfulness (mercury less), unrivaled brilliance, speedy exchanging, variety virtue, and ecological neighborliness. These benefits can supplant the current glowing and fluorescent lights.

As authoritative physical evidence, latent fingerprints (LFPs) have been used for a long time to provide additional donor information like gender, the presence of human metabolites, and evidence of explosive contact. Due to their low optical contrast, LFPs are difficult to see with the naked eye in the majority of cases. As a result, sophisticated methods are required to enable their detection. To date, various strategies have been used to recognize LFPs, particularly powder dusting, metal deposition, cyanoacrylate/iodine fuming, fluorescence

staining, and so on. Among these strategies, powder dusting is the straightforward viable strategy for LFP discovery on assorted surfaces.

Cerium oxide is an oxide of the rare earth metal cerium, also known as ceric oxide, ceria, cerium oxide, or cerium dioxide. It is a white, light-yellow powder having the chemical composition CeO_2 [6]. It is a semiconductor with a wide range of applications in pathology, biomedicine[7], sensors, fuel cells, and catalysis. CeO_2 nanoparticles, a cubic fluorite-type structured ceramic material, exhibit no known crystallographic change (2700°C). Due to their redox reactions, long-lasting stability, and affordability, it's been established that cerium oxide Nanoparticles are excellent catalysts [8].

Gomutra is not a waste material [9]. Gomutra consists of 95% water, 2.5% urea, and the remaining 2.5%, a mixture of salts, minerals, hormones, and enzymes[10].

The cerium oxide nanoparticles are synthesized by a variety of techniques such as the hydrothermal method[11], combustion method[12], microwave technique[13], sol-gel method[14], and co-precipitation method [15] etc. Amongst these, the combustion method was becoming more significant because of its low cost, less time-consuming synthesis, and high yield[16].

The current work examines the CeO_2 nanoparticles synthesized via an eco-friendly combustion route using cow urine as fuel. The characterization techniques are PXRD, DRS, PL, and TEM. Photoluminescence properties and latent fingerprints have also been studied[17].

2. Materials and Methods

Cerium nitrate was used as a precursor, and cow urine was used as fuel. The synthesis of CeO_2 nanoparticles involves many methods, but we chose the combustion method, which is convenient and economically friendly. Cerium nitrate(2.1 g) was dissolved into the reaction solution in 5 ml of distilled water and 15 ml of cow urine. Reaction mixture with stirring for 30 min to get a homogeneous solution. This mixture is then kept in a pre-heated muffle furnace at 500°C . The entire combustion process for producing CeO_2 nanoparticles is completed within 5 min. The mixture gets decomposed into a large number of liberated gases, usually oxygen and nitrogen (H_2O , CO_2 , N_2). The entire process was completed within 5 minutes, and this led to the development of CeO_2 nanoparticles.

3. Results and Discussion

3.1. Powder X-ray diffraction (PXRD).

Figure 1 shows the PXRD pattern of CeO_2 nanoparticles. The characterized peaks are noticed at 2θ angles 28° , 32.5° , 47.5° , and 57° corresponding to the hkl planes (100), (200), (220) and (222). All the diffraction peaks were indexed to cubic fluorite structure and well matched to JCPDS card No. 81-0792[18].

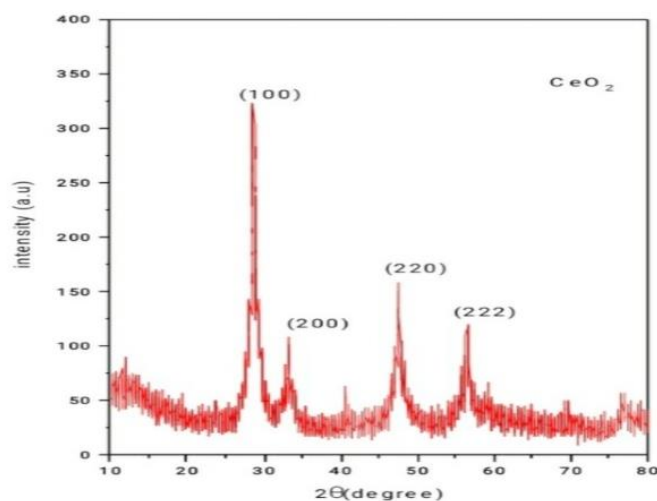


Figure 1. The Powder X-ray diffraction(PXRD) pattern of CeO₂ nanoparticles.

3.2. Transmission electron microscope (TEM).

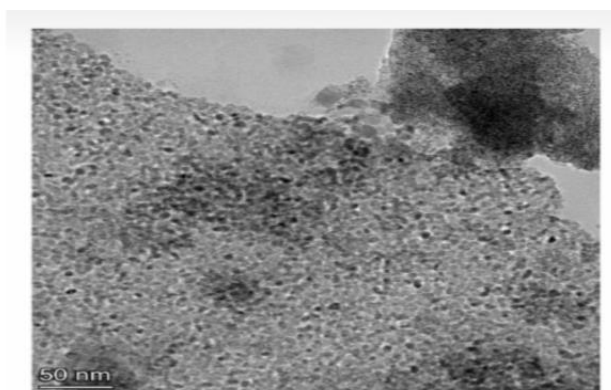


Figure2.TEM image of CeO₂ Nanoparticles

The size and shape of the nanoparticles were determined using transmission electron microscopy. Figure 2 shows the TEM image of CeO₂ nanoparticles. TEM image shows that CeO₂ nanoparticles are spherical. The average particle size of the CeO₂ nanoparticles in the TEM image is 50 nm [19].

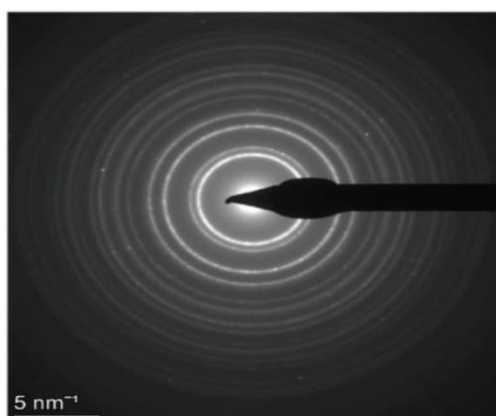


Figure3.SAED patterns of CeO₂ nanoparticles.

Figure 3. shows SAED patterns of CeO₂ nanoparticles. It is used to determine the d – d-spacing of the crystal planes in a single or polycrystalline structure. In the above figure of “SAED,” different rings represent the number of peaks corresponding to PXRD, whereas the higher sharp peaks show less intensity diffraction rings[20]. The four diffraction rings

correspond to miller indices (100), (200), (220), and (222) of lattice planes with reciprocal lattice at [5nm⁻²].

3.3. Diffuse reflectance spectra (DRS).

Diffuse Reflectance Spectra Analysis is used to find nanoparticles' energy gap (E_g) [21]. Figure 4 shows the DRS spectra of CeO₂ nanoparticles. The Kubelka –Munk function was used to determine the energy band gap. The Kubelka–Munk function F (R_∞) and band gap energy (hν) were estimated by utilizing the following equations:

$$F(R_{\infty}) = \frac{(1-R_{\infty})^2}{2R_{\infty}} \quad (1)$$

$$h\nu = \frac{1240}{\lambda} \quad (2)$$

where R_∞ is the reflection coefficient of the sample, and λ is the absorption wavelength. The energy band gap of CeO₂nanoparticles is found to be 3.1eV.

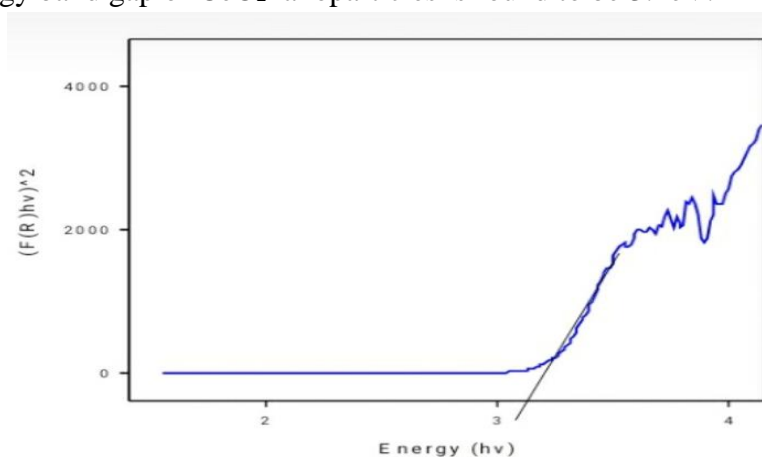


Figure 4. DRS spectra of CeO₂ nanoparticles.

3.4. Photoluminescence(PL).

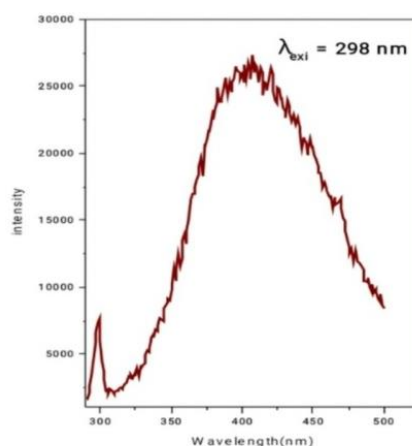


Figure 5. Photoluminescence emission spectra of CeO₂ nanoparticles.

PL is generally used to assess the effectiveness of the charge carrier entrapment, migration, and transfer in addition to comprehending the end of the electron-hole pairs in semiconductors. Figure 5 shows the PL emission spectra of CeO₂ nanoparticles recorded at an excitation wavelength of 298nm. They also observed blue light emission peaks at 300, 350, and 410nm [22].

3.5. Commission International De I-Eclairage (CIE).

Figure 6 shows the Commission International De I-Eclairage (CIE) chromaticity diagram of CeO₂ nanoparticles. The three primary fundamental colors, green, blue, and red, are associated with the chromaticity diagram[23]. The color coordinates of CeO₂ nanoparticles were calculated based on the CIE 1931 standard. The chromaticity coordinates of CeO₂ nanoparticles were located in the blue region. This indicates that the present phosphor has a high potential for fabricating blue components of white light.

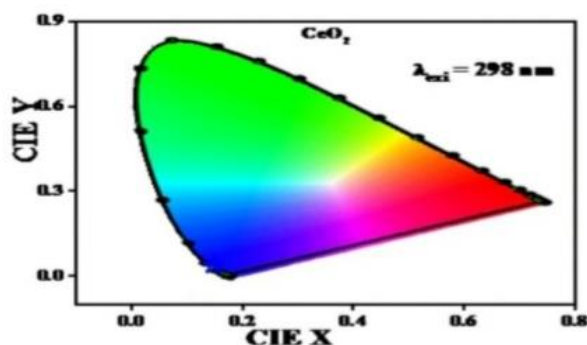


Figure6. CIE chromaticity of CeO₂ nanoparticles.

3.6. Latent fingerprints.

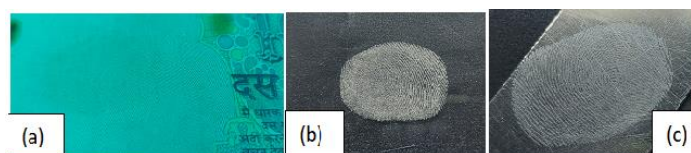


Figure7. LFPs stained by CeO₂ nanoparticles on different materials (a) 10 rupee notes; (b) glass slide; (c) metal scale.

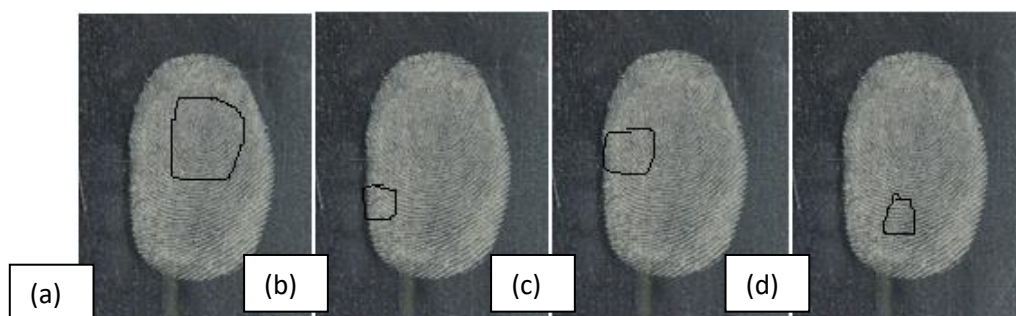


Figure8. LFPs stained by CeO₂ nanoparticles on Glass slide a) whorl; b) bridge; c) bifurcation ;d) eye.

Using luminescent material to detect LFPs was a unique technique because phosphor particles remained attached to the fingerprint residue [24]. CeO₂ nanoparticles are used to stain the fingerprints using a soft feather brush. The LFPs are then visualized under 254 nm UV light or normal light at that point[25]. A series of experiments were carried out on 10 rupee notes, a Glass slide, and a Metal Scale, as shown in Figure 7. It is observed from Figure 8 that the Fingerprints dusted with CeO₂ Nanoparticles show well-defined ridge details like Whorl, Bridge, Bifurcation, and eye. In Figure 8 (a) and (b), level 1 characteristics such as Whorl and Bridge are found. In Figures 8(c) and 8(d), level 2 features of bifurcation and eye are found.

4. Conclusions

The prepared CeO₂ nanoparticles were synthesized by combustion using fuel as cow urine. The obtained CeO₂ Nanoparticles were well characterized by PXRD, DRS, PL, TEM, and SAED techniques. The PXRD pattern shows that the CeO₂ Nanoparticles are cubic fluorite structures. The TEM image shows that it is spherical. SAED pattern shows that CeO₂ nanoparticles are crystalline structures. The estimated energy bandgap of the prepared sample is found to be 3.1eV. The PL emission spectra excited under 298nm exhibit peaks in 300, 350, and 410nm. The CIE coordinates in the blue region. The results obtained demonstrate the suitability of current CeO₂ nanoparticles for advanced forensic and display applications.

Funding

This research received no external funding.

Acknowledgments

The author, Dr. Amith Yadav H.J., thanks IQAC Davangere University, Davangere, India, for sanctioning seed money.

Conflicts of Interest

The authors declare no conflict of interest.

References

1. Bhuvan Raj, N.; Pavithra Gowda, N.T.; Pooja, O.S.; Sukrutha, S.K.; Purushotham, B.; Nagaswarupa, H.P.; Anil Kumar, M.R.; Surendra, B.S.; Shashi Shekhar, T.R.; Prashantha, S.C. Eco-friendly synthesis of CeO₂ NPs using *Aloe barbadensis Mill* extract: Its biological and photocatalytic activities for industrial dye treatment applications. *J. Photochem. Photobiol.* **2021**, *7*, 100038, <https://doi.org/10.1016/j.jpap.2021.100038>.
2. Malleshappa, J.; Nagabhushana, H.; Sharma, S.C.; Vidya, Y.S.; Anantharaju, K.S.; Prashantha, S.C.; Daruka Prasad, B.; Raja Naika, H.; Lingaraju, K.; Surendra, B.S. *Leucas aspera* mediated multifunctional CeO₂ nanoparticles: Structural, photoluminescent, photocatalytic and antibacterial properties. *Spectrochim. Acta - A: Mol. Biomol. Spectrosc.* **2015**, *149*, 452–462, <https://doi.org/10.1016/j.saa.2015.04.073>.
3. Fu, Z.; Lu, L.; Zhang, C.; Xu, Q.; Zhang, X.; Gao, Z.; Li, J. Fuel cell and hydrogen in maritime application: A review on aspects of technology, cost and regulations. *Sustain. Energy Technol. Assess.* **2023**, *57*, 103181, <https://doi.org/10.1016/j.seta.2023.103181>.
4. Wei, L.; Zeng, L.; Han, M.S.; Li, W.J.; Chen, L.P.; Xu, J.H.; Zhao, T.S. Nano TiC electrocatalysts embedded graphite felt for high rate and stable vanadium redox flow batteries. *J. Power Sources* **2023**, *576*, 233180, <https://doi.org/10.1016/j.jpowsour.2023.233180>.
5. Amin, M.N.; Khan, K.; Sufian, M.; Al-Ahmad, Q.M.S.; Deifalla, A.F.; Alsharari, F. Predicting parameters and sensitivity assessment of nano-silica-based fiber-reinforced concrete: a sustainable construction material. *J. Mater. Res. Tehnol.* **2023**, *23*, 3943–3960, <https://doi.org/10.1016/j.jmrt.2023.02.021>.
6. Nagai, M.; Furutani, Y.; Takehara, H.; Ashida, M.; Okuyama, Y.; Kani, Y. Mechanisms of photoluminescence in cerium oxide pellets with different types of defects. *J. Lumin.* **2023**, *260*, 119859, <https://doi.org/10.1016/j.jlumin.2023.119859>.
7. Yang, G.; Liu, F.; Zhao, J.; Fu, L.; Gu, Y.; Qu, L.; Zhu, C.; Zhu, J.-J.; Lin, Y. MXenes-based nanomaterials for biosensing and biomedicine. *Coord. Chem. Rev.* **2023**, *479*, 215002, <https://doi.org/10.1016/j.ccr.2022.215002>.
8. Horká, H.; Šťastný, M.; Bezdička, P.; Švarcová, S. Determination of methanol-derivatives in drying oils after metal oxide-based dispersive solid phase extraction/QuEChERS clean-up. *J. Chromatogr. A* **2022**, *1681*, 463490, <https://doi.org/10.1016/j.chroma.2022.463490>.

9. Nandisha, P.-S.; Sowbhagya. Bio-mediated synthesis of CuO nano bundles from Gomutra (cow urine): Synthesis, characterization, photodegradation of the malachite green dye and SBH mediated reduction of 4-nitrophenol. *Mater. Sci. Eng.* **2023**, *295*, 116607, <https://doi.org/10.1016/j.mseb.2023.116607>.
10. Ghouri, Z.K.; Barakat, N.A.M.; Kim, H.Y.; Park, M.; Khalil, K.A.; El-Newehy, M.H.; Al-Deyab, S.S. Nano-engineered ZnO/CeO₂ dots@ CNFs for fuel cell application. *Arab. J. Chem.* **2016**, *9*, 219-228, <https://doi.org/10.1016/j.arabjc.2015.05.024>.
11. Hunpratub, S.; Chullaphan, T.; Chumpolkulwong, S.; Chanlek, N.; Phokha, S. Characterization and electrochemical properties of Carbon/CeO₂ composites prepared using a hydrothermal method. *Mater. Chem. Phys.* **2023**, *303*, 127820, <https://doi.org/10.1016/j.matchemphys.2023.127820>.
12. Balamurugan, S.; Ashika, S.A.; Jainshaa, J. Influence of synthesis methods (combustion and precipitation) on the formation of nanocrystalline CeO₂, MgO, and NiO phase materials. *Results Chem.* **2023**, *5*, 100941, <https://doi.org/10.1016/j.rechem.2023.100941>.
13. Shi, Y.; Wang, L.; Wu, M.; Wang, F. Order-of-magnitude increase in rate of methane dry reforming over Ni/CeO₂-SiC catalysts by microwave catalysis. *Appl. Catal. B Environ.* **2023**, *337*, 122927, <https://doi.org/10.1016/j.apcatb.2023.122927>.
14. Choubari, M.S.; Mazloom, J.; Ghodsi, F.E. Supercapacitive properties, optical band gap, and photoluminescence of CeO₂-ZnO nanocomposites prepared by eco-friendly green and citrate sol-gel methods: A comparative study. *Ceram. Int.* **2022**, *48*, 21344-21354, <https://doi.org/10.1016/j.ceramint.2022.04.100>.
15. Shibeshi, P.T.; Parajuli, D.; Murali, N. Study of Fe-doped and glucose-capped CeO₂ nanoparticles synthesized by co-precipitation method. *Chem. Phys.* **2022**, *561*, 111617, <https://doi.org/10.1016/j.chemphys.2022.111617>.
16. Vasudha, M.; Gayathri, D.; Gurum, Soundarya, S.S.; Kavya, M.R.; Nagaswarupa, H.P.; Surendra, B.S.; Shashi Shekhar, T.R.; Ravikumar, C.R.; Basavaraju, N.; Prathap Kumar, C. Synthesis of BMA NPs using aloe vera gel for their electrochemical, biological and photocatalytic studies. *J. Photochem. Photobiol.* **2021**, *6*, 100017, <https://doi.org/10.1016/j.jpap.2021.100017>.
17. Lakshmeesha, T.R.; Sateesh, M.K.; Daruka Prasad, B.; Sharma, S.C.; Kavyashree, D.; Chandrasekhar, M.; Nagabhushana, H. Reactivity of Crystalline ZnO Superstructures against Fungi and Bacterial Pathogens: Synthesized Using *Nerium oleander* Leaf Extract. *Cryst. Growth Des.* **2014**, *14*, 4068-4079, <https://doi.org/10.1021/cg500699z>.
18. Yulizar, Y.; Kusriani, E.; Apriandanu, D.O.B.; Nurdini, N. Datura metel L. Leaves extract mediated CeO₂ nanoparticles: Synthesis, characterizations, and degradation activity of DPPH radical. *Surf. Interfaces* **2020**, *19*, 100437, <https://doi.org/10.1016/j.surfin.2020.100437>.
19. Kumaran, C.; Baskaran, I.; Sathyaseelan, B.; Senthilnathan, K.; Manikandan, E.; Sambasivam, S. Effect of doping of iron on structural, optical and magnetic properties of CeO₂ nanoparticles. *Chem. Phys. Lett.* **2022**, *808*, 140110, <https://doi.org/10.1016/j.cplett.2022.140110>.
20. Zhang, N.; Xu, Y.-J. Aggregation- and Leaching-Resistant, Reusable, and Multifunctional Pd@CeO₂ as a Robust Nanocatalyst Achieved by a Hollow Core-Shell Strategy. *Chem. Mater.* **2013**, *25*, 1979-1988, <https://doi.org/10.1021/cm400750c>.
21. Amith Yadav, H.J.; Eraiah, B.; Nagabhushana, H.; Darshan, G.P.; Daruka Prasad, B.; Sateesh, M.K.; Sharma, S.C.; Hema Prabha, P. Bio-inspired ultrasonochemical synthesis of blooming flower like ZnO hierarchical architectures and their excellent biostatic performance. *J. Sci. Adv. Mater. Devices* **2017**, *2*, 455-469, <https://doi.org/10.1016/j.jsamd.2017.11.004>.
22. Malleshappa, J.; Nagabhushana, H.; Sharma, S.C.; Sunitha, D.V.; Dhananjaya, N.; Shivakumara, C.; Nagabhushana, B.M. Self propagating combustion synthesis and luminescent properties of nanocrystalline CeO₂:Tb³⁺ (1-10 mol%) phosphors. *J. Alloys Compd.* **2014**, *590*, 131-139, <https://doi.org/10.1016/j.jallcom.2013.11.213>.
23. Amith Yadav, H.J.; Eraiah, B.; Nagabhushana, H. Ultrasound assisted sonochemical synthesis of ZrO₂: Eu³⁺ nanophosphor. *AIP Conf. Proc.* **2019**, *2115*, 030100, <https://doi.org/10.1063/1.5112939>.
24. Ashwini, K.R.; Premkumar, H.B.; Daruka Prasad, B.; Darshan, G.P.; Nagabhushana, H.; Sharma, S.C.; Prashantha, S.C. Sm-SrAl₂O₄ Nanomaterial: Intensive Orange-red component for white LED, Latent finger Print, and anti-counterfeiting application. *Chem. Phys.* **2022**, *568*, 111799, <https://doi.org/10.1016/j.chemphys.2022.111799>.
25. Amith Yadav, H.J.; Eraiah, B.; Nagabhushana, H.; Darshan, G.P.; Daruka Prasad, B.; Sharma, S.C.; Premkumar, H.B.; Anantharaju, K.S.; Vijayakumar, G.R. Facile Ultrasound Route To Prepare Micro/Nano

Superstructures for Multifunctional Applications. *ACS Sustainable Chem. Eng.* **2017**, *5*, 2061-2074, <https://doi.org/10.1021/acssuschemeng.6b01693>.